

Received 5 August 2024, accepted 15 August 2024, date of publication 19 August 2024, date of current version 2 September 2024.

Digital Object Identifier 10.1109/ACCESS.2024.3446313

RESEARCH ARTICLE

Low-Cost Multiband Four-Port Phased Array Antenna for Sub-6 GHz 5G Applications With Enhanced Gain Methodology in Radio-Over-Fiber Systems Using Modulation Instability

HASSAN ZAKERI¹, RASUL AZIZPOUR¹, PARSA KHODDAMI¹,
GHOLAMREZA MORADI¹, (Senior Member, IEEE),
MOHAMMAD ALIBAKHSHIKENARI², (Member, IEEE),
CHAN HWANG SEE³, (Senior Member, IEEE), TAYEB A. DENIDNI⁴, (Fellow, IEEE),
FRANCISCO FALCONE⁵, (Senior Member, IEEE), SLAWOMIR KOZIEL^{6,7}, (Fellow, IEEE),
AND ERNESTO LIMITI⁸, (Senior Member, IEEE)

¹Department of Electrical Engineering, Amirkabir University of Technology (Tehran Polytechnic), Tehran 158754413, Iran

²Department of Signal Theory and Communications, Universidad Carlos III de Madrid, Leganés, 28911 Madrid, Spain

³School of Engineering and the Built Environment, Edinburgh Napier University, EH10 5DT Edinburgh, U.K.

⁴Centre-Energie Matériaux et Télécommunications, Institut National de la Recherche Scientifique, Montreal, QC H5A 1K6, Canada

⁵Department of Electrical, Electronic and Communication Engineering, and Institute for Smart Cities (ISC), Public University of Navarre, 31006 Pamplona, Spain

⁶Faculty of Electronics, Telecommunication and Informatics, Gdańsk University of Technology, 80-233 Gdańsk, Poland

⁷Department of Engineering, Reykjavik University, 102 Reykjavik, Iceland

⁸Electronics Engineering Department, University of Rome "Tor Vergata," 00133 Rome, Italy

Corresponding authors: Mohammad Alibakhshikenari (mohammad.alibakhshikenari@uc3m.es) and Ernesto Limiti (limiti@ing.uniroma2.it)

Dr. Mohammad Alibakhshikenari acknowledges support from the CONEX (CONnecting EXcellence)-Plus programme funded by Universidad Carlos III de Madrid and the European Union's Horizon 2020 research and innovation programme under the Marie Skłodowska-Curie grant agreement No. 801538.

ABSTRACT Phased array antenna (PAA) technology is essential for applications requiring high gain and wide bandwidth, such as sensors, medical, and 5G. Achieving such a design, however, is a challenging and intricate process that calls for precise calculations and a combination of findings to alter the phase and amplitude of each unit. Furthermore, coupling effects between these PAA structure elements can only be completed with the use of full-wave electromagnetic simulation tools. Due to recent advances, radio-over-fiber (RoF) technology has been positioned as a possible alternative for high-capacity wireless communications. This paper presents a low-cost, multiband Sub-6 GHz 5G PAA with enhanced gain achieved through integration with a new specialized RoF system design to improve PAA performance by using the phenomenon of modulation instability (MI). Optimizing the antenna's Defected Ground Structure (DGS) leads to even more improvement. To enable operation across three distinct frequency bands (Sub-6 GHz n78 band (3-3.8 GHz), n79 band (3.8-5 GHz), and n46 band (5-5.5 GHz)), the proposed antenna design features four elliptical patches strategically positioned at the four sides of the ground plane, providing comprehensive 360° coverage in the azimuth plane. Additionally, integrating elliptical slots and upper gaps contributes to improvement. The proposed PAA's experimentally validated gain values are 5.2 dB, 7.4 dB, and 7.8 dB in the n78, n79, and n46 bands, respectively. For improving the performance of the proposed PAA

The associate editor coordinating the review of this manuscript and approving it for publication was Feng Wei.

in RoF systems, anomalous fibers ($n_2 \neq 0$ and $\beta_2 < 0$) are employed to consider the modulation instability (MI) phenomenon, which can lead to the generation of the MI gain on the carrier sideband. The true time delay (TTD) technique controls the beam pattern by adjusting the time delay between adjacent radiation elements. Furthermore, the TTD technique utilizes frequency combs for the proposed 4-element array antenna to apply MI gain to all antenna elements.

• **INDEX TERMS** Phased array antenna, modulation instability, radio-over-fiber, sub-6 GHz band.

I. INTRODUCTION

Wireless communications, such as LTE and Wi-Fi, typically rely on Sub-6 GHz frequency ranges due to their mobility and effectiveness in indoor environments. However, the proliferation of high-tech devices such as mobile phones, tablets, and smartphones has led to a significant surge in data traffic across wireless networks [1], [2], [3]. To provide incomparable spectrum and broadband services, communication technology is advancing toward its fifth-generation (5G), which will utilize millimeter wave (mm-wave) frequency bands [4], [5], [6], [7]. Multiple-port antennas have recently been suggested for Sub-6 GHz to enhance data rates. However, they require additional support to attain satisfactory gain or sufficient bandwidth (BW) [8], [9], [10], [11].

One of the fundamental challenges in 5G transmission is that phased array antenna (PAA) configurations can considerably increase data rate and capacity over single-port antennas. The upcoming 5G radio access networks are planned to support multiple connections simultaneously while operating over a wide range of frequencies by keeping low latency and acceptable BW [12], [13], [14], [15].

The PAA project aims to design an antenna with high efficiency and broadband performance for various uses, including 5G applications. Only full-wave electromagnetic simulation tools may be used to provide accurate computation and a combination of results acquired for modifying the phase and amplitude of each unit and coupling effects between these elements of the PAA structure. This comes with a well-known downside of forward EM modeling of microwave stages: a notable increase in the computational cost of the design process [16], [17].

In order to achieve both wide coverage and high gain, the PAA system with multi-beam antennas is the best option for 5G wireless systems and mobile terminals [18], [19]. Multiple beams and respectable coverage performance can be achieved with the PAA system; however, some important considerations include the cost of the transmitter/receiver (T/R) modules and the intricacy of the PAA hardware design. Low profile and low fabrication cost feed networks are essential for large-scale PAA system deployment and practical use [20], [21]. Numerous techniques have been employed to generate improved phased array antennas with large-angle scanning capability [22], [23], [24], [25], [26], [27], [28]. Initially, extending the radiation element pattern of the array is a useful technique to enhance the scanning coverage of phased arrays [25]. Techniques like the metal-cavity [29], unique structures and metal via [30], using metal walls [27],

designing the tapered slot [25], and proposing a resonant microstrip meander line [31] are applied to extend the radiation element pattern. Secondly, pattern reconfigurable modern technology efficiently measures phased arrays with large scanning coverage improvement [26], [27]. Thirdly, the mutual coupling among the array elements is crucial to achieving large-angle scanning capability in linear or planar arrays [31]. Antenna performance has been enhanced through various efforts for 5G applications. Researchers aim to design small, highly effective, and low-cost PAAs to operate within the Sub-6 GHz frequency range [32], [33], [34]. In 5G applications, the BW of the antenna plays a crucial role in boosting channel capacity. In [32], a 136 mm \times 68 mm antenna is presented. The design uses a monopole configuration and operates within the 5.15–5.925 GHz frequency range.

The antenna system has been developed in [35] for integrated cognitive radios. However, in this research, the orthogonal positioning of antenna elements inherently improves the isolation between the ports, but the reflectors improve the isolation between the ports by drastically increasing the antenna system's size.

According to [36], a C-shaped antenna with a dimension 20 \times 15 mm² is designed for WLAN and 5G applications. Even though this antenna is small in size which is one of the important characteristics for 5G application, the scattering characteristics are simulated at -6dB. As per industry requirements and upcoming standards like IEEE 802.11ax, it is not a regular practice to accept scattering characteristics at -6dB. Also, the gain of the antenna is not acceptable for a 5G wireless application.

Therefore, designing an antenna with an acceptable gain and a low profile is crucial for the generation of new wireless communication. As in [37], the size of the proposed design noted is 130 mm \times 100 mm with an operating band of 5.1–6 GHz. The gain obtained ranges from 2.5–4.2 dB within the operating frequency band.

A center-fed circular patch antenna is proposed in [38] with shorting posts that can switch between four linear polarizations at a 45° rotation and a broadside beam. Four shorting posts are positioned at a 45° angle to enable rotatability of the linear polarization and the connection between the shorting posts, and four PIN diodes regulate the ground. Turning the PIN diodes ON and OFF allows the patch antenna to alternate between four linear polarizations at a 45° rotation. The 2.4 GHz band can be covered by the measured

overlapping impedance bandwidth of 2.33 GHz to 2.50 GHz for all four polarization states.

A circular disc microstrip-fed monopole antenna with a reconfigured wideband to narrowband frequency is presented in [39]. A reversible band-pass filter was integrated with the antenna in the feed line. An active element could change the impedance bandwidth from wideband to narrowband. Two varactor diodes have been used for the narrowband state to continuously isolate and tune the antenna response between 3.9 and 4.7 GHz.

A monopole antenna with enhanced impedance is proposed in [40]. This antenna covers an acceptable 5G frequency band. However, the size of the antenna is large which limits functionality for 5G applications.

The gain of a PAA is a crucial parameter that significantly influences its performance. A 150 mm × 75 mm antenna with an operational bandwidth of 5.15–5.85 GHz and peak gain of 4.62 dB is proposed in [41]. Researchers in [42] used the defected ground structure (DGS) to raise the gain of the PAA. In the [43], the Photonic Band Gap (PBG) was utilized to improve antenna radiation characteristics.

RoF has recently become one of the most well-known schemes in the communication industry. The RoF systems operating in the Sub-6 GHz range can be employed in wireless access networks, helping to provide high-capacity and low-latency connectivity to support many users, especially in densely populated areas for 5G applications [44], [45], [46]. In that case, the signals can be transported over long distances without suffering significant degradation or loss of quality by utilizing the low-loss properties of fiber optic cables [47], [48].

characteristics, the generated sidebands can be used for different purposes. MI can be created by employing non-linear and anomalous fibers, which can amplify the carrier's sideband. Through pulse modulation and manipulation of the fiber's properties, the input pulse can be positioned within the amplified sideband, exploiting its benefits. Consequently, this approach enhances the system's overall gain [49], [50].

TTD is a crucial technique used in PAAs to control the phase shift among the elements of the array antenna. It refers to the precise and independent adjustment of the time delay applied to each element's signal to steer the antenna's beam in a specific direction. This enables the PAA to form and direct the radiation pattern to a desired target or point of interest. One of the best methods of implementation of TTD is utilizing frequency combs. Upon passing through the fiber, the combs' free spectral range (FSR) is one of the parameters that determines the time delay required to reach the desired beam.

This proposed work presents a low-design complexity, low-cost, and multiband PAA aimed at achieving wideband gain enhancement. Firstly, four printed elliptical patch antennas with tapered feeding are designed and investigated. The design uses a tapered feed, a DGS structure, and a four-slotted elliptical patch to improve wideband performance. The design employs a standard elliptical radiator. To enhance the bandwidth and matching, the above traditional elliptical antenna is modified by adjoining the rotated patch copy to employ the PAA better. Incorporating the elliptical slot helps extend the current path length without modifying the actual dimensions of the antenna. The proposed structure's main highlights are its acceptable gain and multi-bandwidth, which are achieved by enhancing the radiator's electrical length. The elliptical array patch antenna, designed to offer appropriate gain, emerges as a promising candidate for 5G wireless communication applications.

Furthermore, we introduce a novel RoF system that leverages the MI phenomenon to control and amplify the beam of the proposed PAA. Through the utilization of MI, we can modulate the input Sub-6 GHz signals onto the amplified sideband of the carrier, effectively operating within the desired frequency band for signal amplification. This method has been extended to frequency combs. Therefore, all antenna elements can experience an advantage from MI gain. As a result, the performance of PAAs, such as the gain, will be enhanced. Furthermore, we introduce a bit-controlled system that can control the beam angle of the array antenna.

The rest of this paper is composed as follows: Section II discusses the theory and design of the proposed PAA. Section III shows the proposed antenna results. To verify the simulation results, the antenna is experimentally fabricated and measured using the antenna measurement system. In Section IV, a new RoF system is introduced, leveraging fibers under the MI phenomenon that are capable of integrating with the proposed antenna to enhance its performance. Finally, Section V provides a summary of the main results presented in this paper.

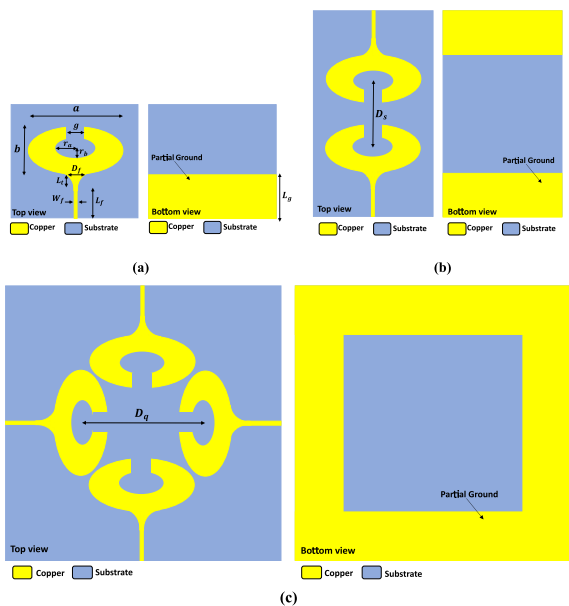


FIGURE 1. The progression of the proposed PAA design for 5G wireless application.

RoF systems benefit from MI in specific applications. By controlling system parameters and utilizing MI's

MOST WIEDZY Downloaded from mostwiedzy.pl

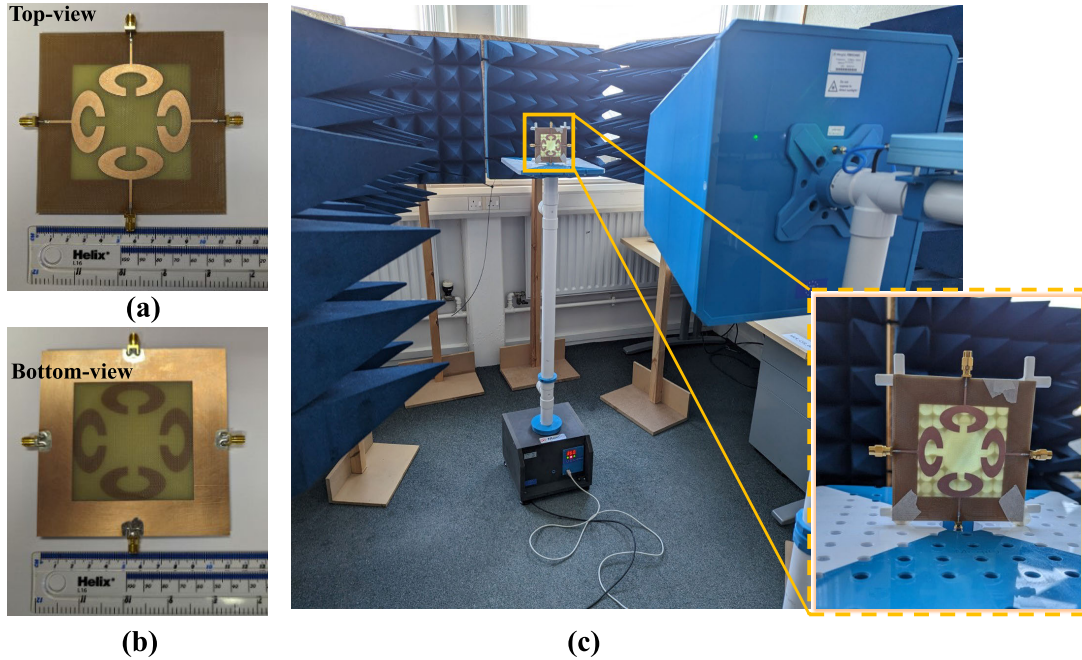


FIGURE 2. Fabricated prototype of the proposed PAA structure for 5G wireless application a) top view b) bottom view c) measurement setup.

TABLE 1. Dimensions of the proposed elliptical patch antenna.

Parameters	<i>a</i>	<i>b</i>	<i>r_a</i>	<i>r_b</i>	<i>g</i>	<i>D_f</i>	<i>L_t</i>	<i>W_f</i>	<i>L_f</i>	<i>D_s</i>	<i>D_q</i>	<i>L_g</i>
Value (mm)	49.3	19.5	12.5	5	4.4	3.4	2.6	1.6	18.3	32.7	51.5	20.9

II. PAA-ANTENNA THEORY AND DESIGN

The elliptical patch is considered one of the best candidates and the simplest shape of microstrip patch antenna applied in wireless technology to achieve high BW. The elliptical shape has several advantages, like having more degrees of freedom than the circular geometry and providing larger flexibility in the design [51], [52].

For an elliptical patch shape of a major axis and a minor axis, the perimeter is given by:

$$p = 2aE(em) \tag{1}$$

where $E(em)$ is the elliptic integral of the second kind with elliptic modulus em , the eccentricity.

The size and axial ratio of the elliptical patch are determined by using approximate formulas given by [53], [54], [55]

$$em = \sqrt{1 - \left(\frac{b}{a}\right)^2} \tag{2}$$

and

$$f_r = \frac{c}{p\sqrt{\epsilon_r}} \tag{3}$$

Here, c and ϵ_r are the light's speed and the dielectric substrate's relative permittivity, respectively.

The elliptical slot and the adjusted gap are employed for better BW and increase the peak gains, and the truncation is used between the microstrip line and elliptical patch for

having a good impedance [56], [57], which helps to be good candidates for Sub-6 GHz in 5G wireless technology.

Fig. 1 demonstrates the progression of the design of the PAA. Initially, single radiating patch elements are designed followed by 2×1 and 2×2 PAAs to achieve better gain.

The design evolved from the basics of a mono-patch antenna. The antenna consists of the patch section, tapered feed region, and DGS section. The tapered feedline and the elliptical patch improve the antenna performance and matching. The tapered feedline concatenated with the main patch aids in smoothening the current path, resulting in a broader impedance bandwidth. Hence, this mono patch antenna is fed by a tapered curve feed line, optimized to 50Ω impedance matching to reduce incident wave reflection. As result, tapered feed line's width at the bottom end corresponds to a characteristic impedance of 50Ω , and the width at the top end has a characteristic impedance of 75Ω . The tapered feed line, together with the mono-patch antennas, tends to have enhanced bandwidth performance and can transmit UWB pulses with minimal distortion

Using a PAA configuration helps reduce coupling effects and improve spatial and pattern diversity. Copper was used to create the radiating element, which has a highly stable conductivity of $5.8 \times 10^7 S/m$. This stability resulted in minimal impact on the impedance matching. The parameters are optimized by using CST microwave studio as commercial software.

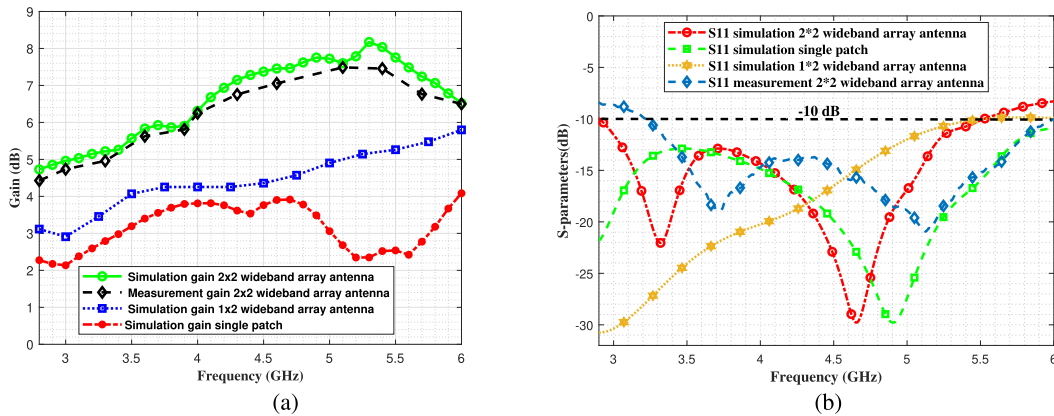


FIGURE 3. Development of simulated and measured results of the wideband microstrip PAA: (a) gain (b) reflection coefficient (S11).

The characteristics of the substrate, such as the tangent loss ($\tan(\delta)$), the dielectric constant, and height, have a significant impact on the impedance matching and BW of an antenna. A very thin substrate may result in high copper losses, but a thicker substrate may reduce the antenna's performance due to surface waves. To achieve a suitable impedance matching, the proposed antenna is mounted on the low-cost FR-4 substrate with a dielectric constant of $\epsilon_r = 4.3$, a loss tangent of $\tan(\delta) = 0.025$ and a thickness of 0.787 mm. Table 1 demonstrates the parameters of the suggested antenna. The parameters are optimized for the proposed PAA to achieve resonance frequency ranges from 2.9 GHz to 5.3 GHz and to guarantee reduced mutual coupling between antenna parts.

The design evolution begins with a conventional elliptical patch, as Figure 1 depicts. The design first provided a simple elliptical patch with bandwidth for a 5G application and three stop bands. As the evolution proceeds towards the second stage, a central elliptical slot with a smaller upper gap is created to increase the bandwidth and gain. These values are improved for mono-patch by optimizing initially the r_a and r_b for bandwidth and then g for gain, respectively. A small curved transition microstrip line connects the patches to the feed line is added to have good impedance matching and decrease the reflection coefficient [1]. The 1×2 antenna is designed for the next stage. The distance between the patches directly affects the proposed structure's directivity. Finally, the final structure is designed for the 5G wireless application. In this stage, the value of the L_g is optimized to reduce the side lobe levels.

III. SIMULATION AND MEASURED RESULTS

This section presents and discusses the simulation and measured results of the proposed PAA. The simulation is conducted using CST Microwave Studio, which is an electromagnetic simulation software available commercially. Fig. 2 demonstrates the prototype of the proposed structure. Measurement of all the radiation performance was carried out in an anechoic far-field chamber.

The reflection coefficient S_{11} and realized gain for each stage of the antenna's development are shown in Fig. 3.

Accurately designing and increasing the radiating elements clarifies how it impacts the antenna's performance. Good agreement between the simulated and measured results can be observed. The realized gain of the first and second stages varies between 1.9 and 4.5 dB across the frequency operating range from 3 GHz to 5.5 GHz, as shown in Fig. 3(a). Meanwhile, the suggested 2×2 PAA achieved a realized gain of 5 to 8.1 dB throughout the operational spectrum. The measured gain variation is less than 2 dB within this operational band. However, due to minor fabrication and measurement inaccuracy issues, the measured gain is slightly higher than the simulated result at certain frequencies. Additionally, as illustrated in Fig. 3(b), these antennas have low reflection coefficients (S11), less than -10 dB in both simulation and measured results. Furthermore, for the suggested PAA to function effectively, all other S-parameters must remain below -10 dB. Fig. 7 demonstrates the measurement and simulation of the transmission and reflection coefficients of the proposed PAA.

Optimizing the distances and dimensions of the radiation elements improves the PAA's performance, helping to achieve resonance frequencies of 3.3 GHz, 4.6 GHz and 5.2 GHz.

Fig. 4 demonstrates the radiation patterns in the magnetic field (H) plane and electrical field (E) plane at three frequencies 3.3 GHz, 4.6 GHz, and 5.2 GHz.

A 3D radiation pattern is a graphical representation of the radiated power from an antenna in free space, achieved in the far-field region. It provides a three-dimensional view of how the antenna's power is distributed in different directions.

The 3D radiation patterns of the antenna proposal are displayed in Fig. 5. The maximum directivity at 3.3 GHz, 4.6 GHz, and 5.2 GHz are 5.2 dB, 7.4 dB, and 7.8 dB, respectively. These results demonstrate that the proposed PAA exhibits favorable radiation patterns at three different frequencies, making it well-suited for Sub-6 GHz 5G wireless applications.

To reveal the working mechanism, Fig. 6 displays the distribution of the surface current on the YoX cutting plane above the surface of the PAA at these frequencies. The current has a high strength near the patch and feed intersection. Fur-

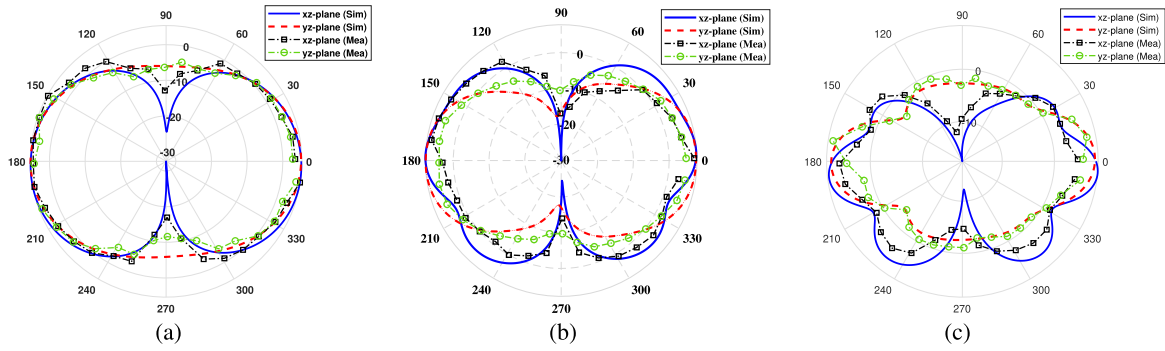


FIGURE 4. The simulated and measured E-field and H-field radiation patterns of the wideband PAA at (a) 3.3 GHz, (b) 4.6 GHz, and (c) 5.2 GHz.

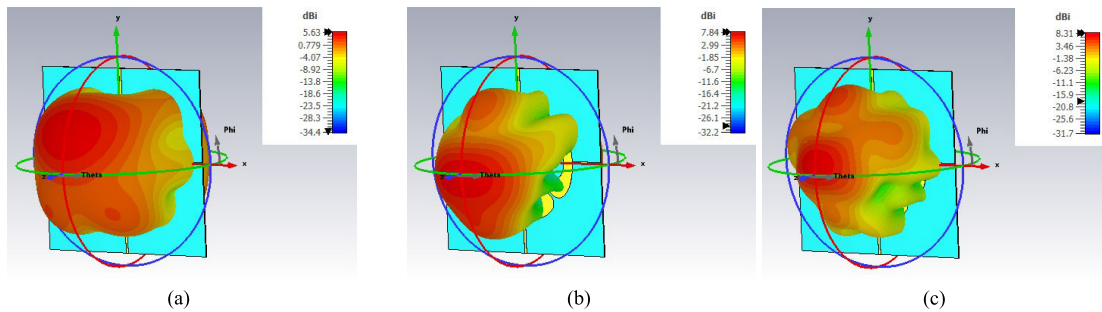


FIGURE 5. The 3D simulated pattern of the proposed PAA at (a) 3.3, (b) 4.6, and (c) 5.2 GHz.

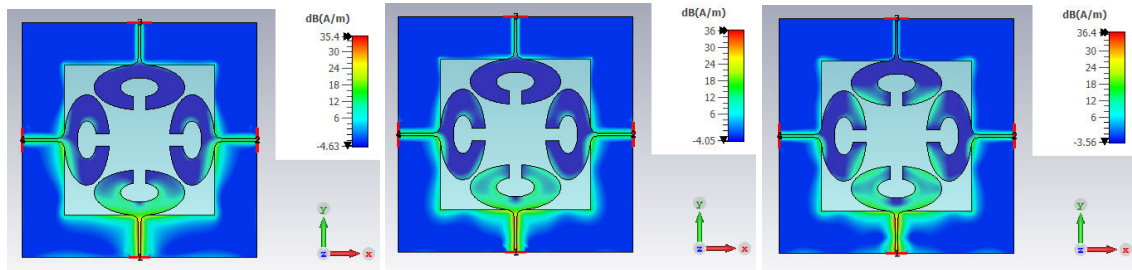


FIGURE 6. Surface current distribution of the proposed PAA at (a) 3.3, (b) 4.6, and (c) 5.2 GHz.

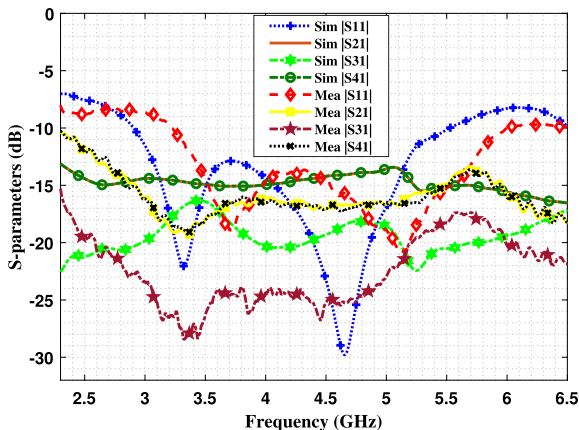


FIGURE 7. Simulation and measured transmission and reflection coefficients of the proposed PAA.

thermore, the level of coupling among the elements is quite negligible, as indicated by the current distribution pattern.

Table 2 demonstrates the comparison of the proposed antenna with other Sub-6 GHz candidate array antennas for 5G wireless communication applications.

IV. PROPOSED RADIO-OVER-FIBER STRUCTURE

The application of RoF systems in Sub-6 GHz antennas offers several advantages, including enhanced performance, increased coverage, and improved signal quality. RoF technology utilizes optical fibers to transport radio signals, enabling flexible and efficient transmission of data over long distances. When integrated with Sub-6 GHz antennas, RoF systems can extend the reach of wireless communication networks, particularly in urban and indoor environments where signal propagation may be limited. Additionally, RoF systems can facilitate centralized processing and coordination of multiple antennas, leading to optimized network performance and resource allocation [58], [59]. Overall, the application of RoF systems in Sub-6 GHz antennas holds

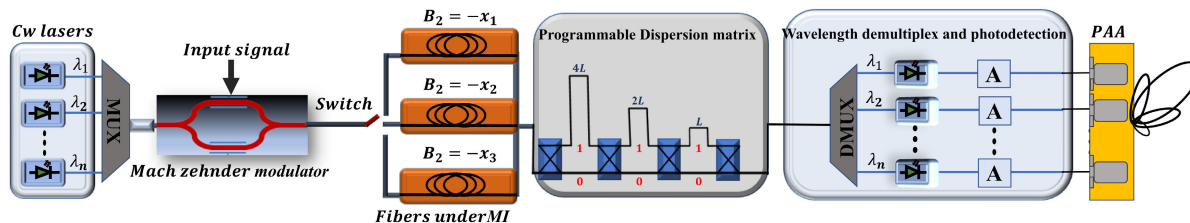


FIGURE 8. RoF diagram with the utilization of optical fiber under MI phenomenon with dispersion coefficients of $x_1 = 60 \text{ ps}^2/\text{km}$, $x_2 = 90 \text{ ps}^2/\text{km}$, and $x_3 = 120 \text{ ps}^2/\text{km}$.

TABLE 2. Comparison features of the suggested PAA with other array antennas.

Ref.	Operational freq. (GHz)	Profile	Bands (GHz)	Peak gain (dB)	Substrate	Cost	Efficiency (%)
[32]	3.1, 5.93	$1.62\lambda \times 0.82\lambda$	0.34, 0.66	2.5, 6.22	FR-4	low	41%-69%
[37]	3.6, 5.7	$1.82\lambda \times 0.9\lambda$	0.4, 0.8	3.5, 5.65	FR-4	low	70%-86%
[41]	3.4, 4.7, 5.4	$1.5\lambda \times 1.1\lambda$	0.4, 0.5, 0.2	3.61, 4.39, 4.62	FR-4	moderate	60%-78%
[62]	0.8, 2	$1.8\lambda \times 0.4\lambda$	0.2, 0.8	4.3, 8.1	FR-4	low	51%-75%
[63]	2.45, 5.2	$1.67\lambda \times 0.833\lambda$	0.4, 0.5	4, 7.1	Rogers 5880	high	85%-92%
[64]	2.6, 4.3	$1.81\lambda \times 1.81\lambda$	0.45, 0.58	4.2, 6.3	Rogers 4350	medium	68%-80%
[65]	2.3, 5.5	$1.69\lambda \times 1.231\lambda$	0.35, 0.75	2.3, 4.2	Rogers 4003	medium	82%-90%
This work	3.3, 4.6, 5.2	$1.07\lambda \times 1.07\lambda$	0.8, 1.2, 0.5	5.2, 7.4, 7.8	FR-4	low	78%-91%

promise for enhancing the capabilities and reliability of wireless communication systems, particularly in the context of emerging 5G networks and IoT applications [60], [61].

The schematic of the proposed RoF system is displayed in Fig. 8. Continuous Wave (CW) lasers excite as the sources of frequency combs, and the input signals undergo modulation through a Mach-Zehnder modulator (MZM). The resulting optical signal is then amplified by passing through non-linear and anomalous fibers ($n_2 \neq 0$ and $\beta_2 < 0$), utilizing the MI phenomenon.

The switch allows the proposed RoF system to operate on the antenna’s desired frequency band. The control section also enables precise manipulation of the antenna beam. Finally, the demultiplexer (DMUX) and photodetectors separate the excitation signals, ensuring each antenna element receives the correct signals.

A. MODULATION INSTABILITY METHOD

MI is a nonlinear phenomenon in the presence of an intense optical carrier wave that travels through a nonlinear medium. It is induced by the interaction between dispersion, nonlinearity, and diffraction. The spectral sidebands are expected to exponentially expand at the output along with the carrier wave’s central band. While the carrier tends to be a CW laser optical beam, rapid fluctuations usually appear as modulated pulse trains [66], [67].

In optical communication, the dispersion of fiber plays an essential role in the transmission of short optical pulses. This is because the numerous spectral components of the pulse travel at different speeds, as indicated by $\frac{c}{n(w)}$.

In order to consider the impact of fiber dispersion, the mode-propagation constant is expanded in a Taylor series around the frequency w_0 where the pulse spectrum is centered. Below is the equation that represents this concept:

$$B(w) = \sum_{m=0}^{\infty} \frac{B_m}{m!} (w - w_0)^m \tag{4}$$

where $\beta(w)$ can be expanded in a Taylor series around w_0 , and β_m represents the dispersion parameter of order m .

Here is the non-linear Schrödinger equation that serves as a model for optical pulse propagation:

$$i \frac{\partial A}{\partial z} + i \frac{\alpha}{2} A - \frac{\beta_2}{2} \frac{\partial^2 A}{\partial T^2} + \gamma |A|^2 A = 0 \tag{5}$$

where γ , A , α , and β_2 represent the non-linear parameter, the slowly varying envelope of the optical pulse, the loss factor of the fiber, and the dispersion of the group velocity, respectively.

When the time-dependent derivation is ignored, eq. 5 is simply solved to yield the steady-state continuous radiation solution. The CW for the eq. 5 is a soliton with the form $\sqrt{P_0} e^{i\gamma P_0 z}$, in the case of the lossless response of the laser, that P_0 is the incident power and $\phi_{NL} = \gamma P_0 z$ is the non-linear phase shift induced by self-phase modulation.

If the steady-state is stable against small perturbations in the power of the laser, the form of is:

$$A = (\sqrt{P_0} + a_1 e^{i(Kz - \Omega t)} + a_2 e^{-i(Kz - \Omega t)}) e^{i\gamma P_0 z} \tag{6}$$

where K and Ω are the wave-number and frequency perturbation at sideband frequency of laser spectrum [67], [68].

By substituting eq. 6 in eq. 5, the following equation can be achieved:

$$K = \pm \frac{1}{2} |\beta_2 \Omega| \left[\Omega^2 + \text{sgn}(\beta_2) \Omega_c^2 \right]^{\frac{1}{2}} \tag{7}$$

which Ω_c has an inverse relation with the non-linear length L_{NL} and the β_2 ($\Omega_c = 2/\sqrt{|\beta_2| L_{NL}}$). When the group velocity dispersion is positive ($\beta_2 > 0$), in all situations, the wave-number (K) is real. Also, the steady-state is stable in all small perturbations. On the other hand, when the group velocity dispersion becomes negative ($\beta_2 < 0$), the wave-number is imaginary, and the perturbation increases.

MOST WIEDZY Downloaded from mostwiedzy.pl

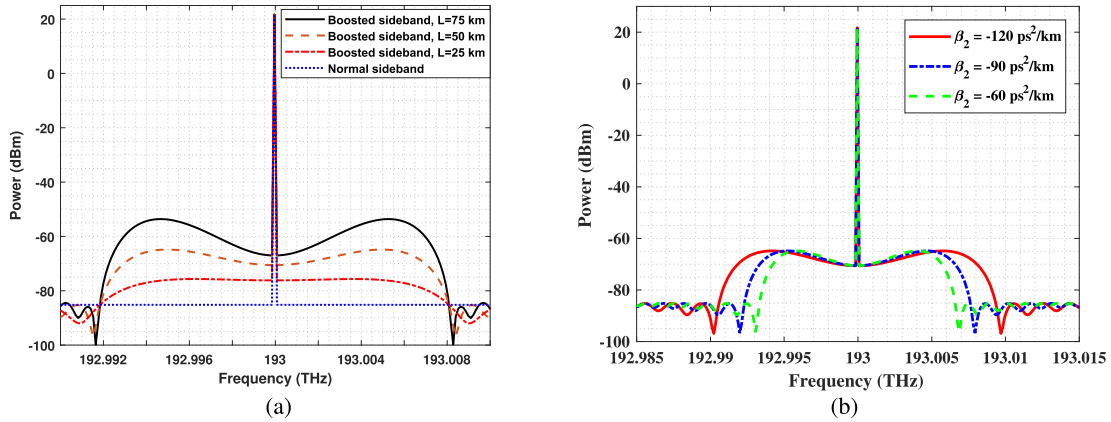


FIGURE 9. a) Unboosted and boosted sideband by different fiber lengths of 25 km, 50 km, and 75 km. b) Boosted sideband by the different values of group velocity dispersion of the fiber.

Therefore, in the negative dispersion, the gain is:

$$G_{MI}(\Omega) = |\beta_2 \Omega| \sqrt{\Omega_c^2 - \Omega^2} \quad (8)$$

The maximum gain also occurs at frequency $\Omega_{max} = \pm \frac{\Omega_c}{\sqrt{2}}$.

Fig. 9 illustrates a comparison between the conventional carrier sideband power and the carrier sideband power under MI. The MI technique can be adapted to operate at different frequency bands by adjusting the fiber parameters. In Fig. 9(a), the amplification is presented for different fiber lengths with the carrier frequency of 193 THz. The maximum MI gain is observed at a frequency shift of $f_{max} = 5$ GHz, which supports Sub-6 GHz 5G communications. Notably, the -85 dBm unboosted sideband experiences significant amplification. As the length of the fiber increases, the MI gain at the sideband carrier also rises. Specifically, for fiber lengths of 25 km, 50 km, and 75 km, the MI gain is 10 dB, 20 dB, and 31 dB, respectively.

In addition, Fig. 9(b) illustrates the sideband amplification under varying fiber group velocities, considering it particularly well-suited for amplifying input signals in Sub-6 GHz applications. Three fibers are utilized in the RoF system to select the appropriate frequency for the proposed array antenna's operating frequency. Hence, with group velocity dispersion of $\beta_2 = -60 ps^2/km$, $\beta_2 = -90 ps^2/km$, and $\beta_2 = -120 ps^2/km$, amplification can be achieved at the range of 3 GHz to 6 GHz. Based on the relations outlined in subsection IV-A, it is evident that the central frequency of the amplification band exhibits an inverse relationship with the group dispersion of the fiber ($f_{max} \propto 1/\sqrt{|\beta_2|}$). Notably, the non-linear refraction index of the fiber and laser power are $n_2 = 0.8 \times 10^{-20} m^2.W^{-1}$ and 300 mW, respectively.

B. TRUE TIME DELAY METHOD

In wideband phased-array antenna (PAA), TTD utilization emerges as a fundamental technique to effectively address beam-steering and beamforming challenges. By employing TTD, several advantages from the optical domain become

feasible, such as wide bandwidth, immunity to electromagnetic radiation, and minimal signal loss.

One of the convenient approaches to implementing TTD in Microwave Photonics (MWP) is using parallel and separate fibers with low dispersion. The time delay variation is determined by the difference in length between the fibers corresponding to each adjacent radiation element in the PAA. However, this method can lead to increased costs and bulkiness due to the requirement of individual fibers to excite each radiation element (multi-fiber structure).

Instead of utilizing multiple fibers with a single source, a more practical approach [69] involves employing a single fiber with a frequency-comb source. These configurations introduce a time delay and dispersion in the fiber due to the differential frequency of the modulated pulses on the adjacent frequency combs.

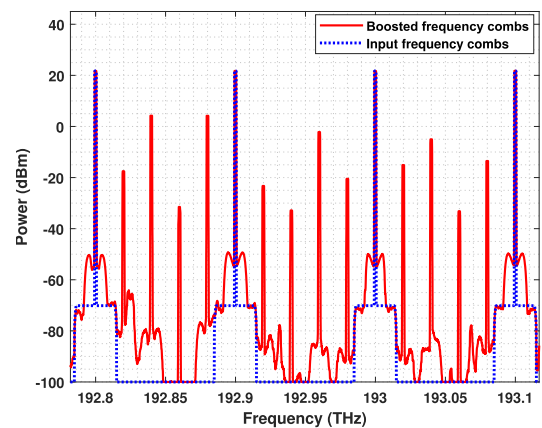


FIGURE 10. Normal and boosted system response frequency combs with FSR of 100 GHz.

Fig. 10 shows the system response when MI is extended to a frequency comb source with the FSR of 100 GHz. The amplified frequency comb serves as the basis for PAA utilizing TTD techniques.

$$\Delta\tau = (|D_{mi}L_{mi}| - |D_cL_c|)\Delta\lambda \quad (9)$$

The relation between the TTD and the length of the fibers is demonstrated in eq. 9, where D_{mi} and L_{mi} are the dispersion and the length of the fibers under MI, respectively. Also, D_c is the dispersion, and L_c is the length of the normal fibers ($\beta_2 > 0$) used in the control system.

The value of the TTD with the FSR of 100 GHz ($\Delta\lambda = 0.8$ nm), assuming the length of fiber equivalent to $L_{mi}=50$ km, is greater than the required time delay of the antenna. To address this, the bit-control system uses the fiber with positive dispersion ($\beta > 0$) to decrease the time delay.

The binary delay line with optical switch components and dispersive fibers provides a basis for the dispersion matrix, as shown in Fig. 8.

Avoiding time delay is also possible by considering $|D_{mi}L_{mi}| = |D_cL_c|$. Therefore, we have developed a configurable dispersion matrix to achieve precise control over the time delay introduced by the fiber under MI.

Using a fiber with positive dispersion ($\beta > 0$) helps to reduce the excessive time delays in PAA and also enables us to control the time delay for PAA by adjusting the minimum time delays.

To optimize the control system's time delay, we consider the minimum and maximum fiber lengths denoted as L and $15L$, respectively. Decreasing either D_c or L_c allows us to increase the time delay as desired.

It is evident from eq. 9 that there are two manners to modify the steering angle. In. Also, it enables changing the FSR, which uses the frequency combs. It is possible to select the appropriate frequency. After that, using eq. 8 as a guide, modifying the fiber length while maintaining the same type. It is notable to note that the second strategy is more accessible with respect to the first one. Following this, the comb line undergoes photo-detection and de-multiplexing processes. Subsequently, the array antenna receives the amplified microwave signals that have been generated.

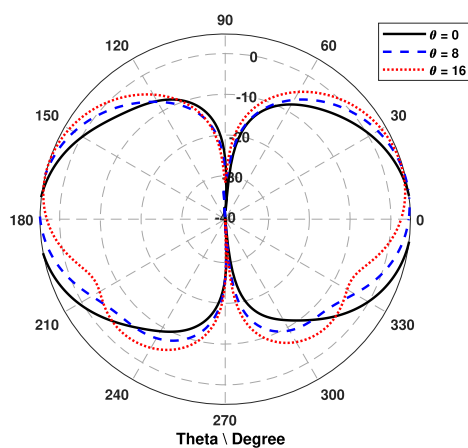


FIGURE 11. Beam steering diagram of the proposed PAA at 3 GHz in three different angle at $\theta = 0$, $\theta = 8$, $\theta = 16$.

The beam angle of an array antenna is determined by its design parameters, including the wavelength of the operating

frequency and the spacing between the antenna elements (d_{PAA}). The formula for calculating the beam angle of an array antenna is as follows:

$$\Theta_0 = \sin^{-1} \frac{c \cdot \Delta\tau}{d_{PAA}} \quad (10)$$

where θ_0 is the radiating steering angle, c is the speed of light in the vacuum space, and $\Delta\tau$ is the time delay.

Beamforming based on TTD in a PAA is essential for communication systems because it demonstrates excellent operating frequency and BW performance. The advantages of low loss and immunity to electromagnetic interference raise wireless communication quality.

Fig. 11 clearly shows the benefits of TTD beam steering by choosing the angle of 0° , 8° , and 16° for the main lobe of the proposed array antenna at 3 GHz. The main lobe's peak can be precisely directed to a specific angle by fine-tuning the antenna's phase offset.

V. CONCLUSION

This work presented a novel design of PAA for 5G wireless applications. The antenna comprises four elliptical patches, each with a central slot and upper gap for simultaneously increasing the BW and gain.

The prototype wideband *twice2* PAA with a low-cost FR-4 substrate is fabricated and measured. The simulation and measured results demonstrate that this antenna has a -10 dB bandwidth of more than 2.5 GHz and covers three essential 5G bands: the n78 band (3)-3.8 GHz, the n79 band (3.8-5 GHz), and the n46 band (5)-5.5 GHz. The realized gains are above 5 dB in the Sub-6 GHz 5G band, while the achieved gains at 4.6 GHz and 5.2 GHz are 7.4 and 7.8 dB, respectively.

We also proposed a new way to improve the antenna performance in Sub-6 GHz 5G applications by using a novel RoF system that employs the MI phenomenon. This proposed model allows the antenna to achieve MI gain, work in a switchable band, and have a tuned beam.

To achieve this goal, non-linear and anomalous fibers ($n_2 \neq 0$ and $\beta_2 < 0$) are employed. The non-linear refraction index of the fiber is $n_2 = 0.8 \times 10^{-20} m^2 \cdot W^{-1}$ and laser power is 300 mW. Three fibers under MI with group velocity dispersion of $\beta_2 = -60 ps^2/km$, $\beta_2 = -90 ps^2/km$, and $\beta_2 = -120 ps^2/km$, are used for maximum amplification in frequency ranges of 2.5-5 GHz, 4-5.5 GHz and 5-7.5 GHz respectively. By employing these fibers, the entire operating frequency range of the PAA can be covered. The MI gain is displayed for fiber lengths of 25 km, 50 km, and 75 km, with values of 10 dB, 20 dB, and 31 dB, respectively.

The TTD technique is used to controls better the beam pattern, by adjusting the time delay between adjacent of the radiation elements.

In conclusion, the proposed system is an acceptable candidate to increase the effectiveness and functionality of

the 5G wireless communication system, with high gain, low complexity, and low-cost structure.

REFERENCES

- [1] S. Shamooun, W. Y. Zhou, F. Shahzad, W. Ali, and H. Subblyal, "Integrated sub-6 GHz and millimeter wave band antenna array modules for 5G smartphone applications," *AEU-Int. J. Electron. Commun.*, vol. 161, Mar. 2023, Art. no. 154542.
- [2] M. E. Morocho-Cayamcela, H. Lee, and W. Lim, "Machine learning for 5G/B5G mobile and wireless communications: Potential, limitations, and future directions," *IEEE Access*, vol. 7, pp. 137184–137206, 2019.
- [3] S. A. Khorasani, H. Zakeri, G. Moradi, M. Alibakhshienari, C. H. See, and E. Limiti, "Orbital angular momentum with the approach of using in sub-6 GHz 5G mobile communications for wireless applications," in *Proc. 6th Global Power, Energy Commun. Conf. (GPECOM)*, Jun. 2024, pp. 1–4.
- [4] E. Bjornson, L. Van der Perre, S. Buzzi, and E. G. Larsson, "Massive MIMO in sub-6 GHz and mmWave: Physical, practical, and use-case differences," *IEEE Wireless Commun.*, vol. 26, no. 2, pp. 100–108, Apr. 2019.
- [5] H. Zakeri, R. S. Shirazi, and G. Moradi, "An accurate model to estimate 5G propagation path loss for the indoor environment," 2023, *arXiv:2302.10057*.
- [6] J. Choi, J. Park, Y. Youn, W. Hwang, H. Seong, Y. N. Whang, and W. Hong, "Frequency-adjustable planar folded slot antenna using fully integrated multithrow function for 5G mobile devices at millimeter-wave spectrum," *IEEE Trans. Microw. Theory Techn.*, vol. 68, no. 5, pp. 1872–1881, May 2020.
- [7] V. Jayaprakash, D. Chandu, R. K. Barik, and S. Koziel, "Compact substrate-integrated hexagonal cavity-backed self-hexaplexing antenna for sub-6 GHz applications," *IEEE Access*, vol. 12, pp. 54397–54404, 2024.
- [8] S. Jabeen and Q. U. Khan, "An integrated MIMO antenna design for sub-6 GHz & millimeter-wave applications with high isolation," *AEU-Int. J. Electron. Commun.*, vol. 153, Aug. 2022, Art. no. 154247.
- [9] R. N. Tiwari, R. Thirumalaiah, V. R. Naidu, G. Sreenivasulu, P. Singh, and S. Rajasekaran, "Compact dual band 4-port MIMO antenna for 5G-sub 6 GHz/N38/N41/N90 and WLAN frequency bands," *AEU-Int. J. Electron. Commun.*, vol. 171, Nov. 2023, Art. no. 154919.
- [10] P. R. Girjashankar and T. Upadhyaya, "Substrate integrated waveguide fed dual band quad-elements rectangular dielectric resonator MIMO antenna for millimeter wave 5G wireless communication systems," *AEU-Int. J. Electron. Commun.*, vol. 137, Jul. 2021, Art. no. 153821.
- [11] I. U. Din, M. Alibakhshienari, B. S. Virdee, S. Ullah, S. Ullah, M. R. Akram, S. M. Ali, P. Livreri, and E. Limiti, "High performance antenna system in MIMO configuration for 5G wireless communications over sub-6 GHz spectrum," *Radio Sci.*, vol. 58, no. 10, pp. 1–22, Oct. 2023.
- [12] O. Semiari, W. Saad, M. Bennis, and M. Debbah, "Integrated millimeter wave and sub-6 GHz wireless networks: A roadmap for joint mobile broadband and ultra-reliable low-latency communications," *IEEE Wireless Commun.*, vol. 26, no. 2, pp. 109–115, Apr. 2019.
- [13] A. Ahad, M. Tahir, and K. A. Yau, "5G-based smart healthcare network: Architecture, taxonomy, challenges and future research directions," *IEEE Access*, vol. 7, pp. 100747–100762, 2019.
- [14] A. Mohanty and S. Sahu, "4-port UWB MIMO antenna with Bluetooth-LTE-WiMax band-rejection and vias-MCP loaded reflector with improved performance," *AEU-Int. J. Electron. Commun.*, vol. 144, Feb. 2022, Art. no. 154065.
- [15] M. A. Tulum, A. S. Turk, and P. Mahouti, "Data driven surrogate modeling of phase array antennas using deep learning for millimetric band applications," *IEEE Access*, vol. 11, pp. 114415–114423, 2023.
- [16] A. K. Vallappil, M. K. A. Rahim, B. A. Khawaja, N. A. Murad, and M. G. Mustapha, "Butler matrix based beamforming networks for phased array antenna systems: A comprehensive review and future directions for 5G applications," *IEEE Access*, vol. 9, pp. 3970–3987, 2021.
- [17] L. Van Messem, A. Moerman, O. Caytan, I. L. de Paula, B. Hoflack, B. Stroobandt, S. Lemey, M. Moeneclaey, and H. Rogier, "A 4×4 millimeterwave-frequency Butler matrix in grounded co-planar waveguide technology for compact integration with 5G antenna arrays," *IEEE Trans. Microw. Theory Techn.*, vol. 71, no. 1, pp. 122–134, Jan. 2023.
- [18] C. Ding, Y. J. Guo, P.-Y. Qin, and Y. Yang, "A compact microstrip phase shifter employing reconfigurable defected microstrip structure (RDMS) for phased array antennas," *IEEE Trans. Antennas Propag.*, vol. 63, no. 5, pp. 1985–1996, May 2015.
- [19] M. Li, S.-L. Chen, Y. Liu, and Y. J. Guo, "Wide-angle beam scanning phased array antennas: A review," *IEEE Open J. Antennas Propag.*, vol. 4, pp. 695–712, 2023.
- [20] P. Xu, Y. Wang, X. Xu, L. Wang, Z. Wang, K. Yu, W. Wu, M. Wang, G. Leng, D. Ge, X. Ma, and C. Wang, "Structural-electromagnetic-thermal coupling technology for active phased array antenna," *Int. J. Antennas Propag.*, vol. 2023, pp. 1–36, Mar. 2023.
- [21] X. Xia, C. Yu, F. Wu, Z. H. Jiang, Y.-L. Li, Y. Yao, and W. Hong, "Millimeter-wave phased array antenna integrated with the industry design in 5G/B5G smartphones," *IEEE Trans. Antennas Propag.*, vol. 71, no. 2, pp. 1883–1888, Feb. 2023.
- [22] K. Hu, Y. Zhou, S. K. Sitaraman, and M. M. Tentzeris, "Additively manufactured flexible on-package phased array antennas for 5G/mmWave wearable and conformal digital twin and massive MIMO applications," *Sci. Rep.*, vol. 13, no. 1, Aug. 2023, Art. no. 12515.
- [23] R. Wang, B.-Z. Wang, C. Hu, and X. Ding, "Wide-angle scanning planar array with quasi-hemispherical-pattern elements," *Sci. Rep.*, vol. 7, no. 1, Jun. 2017, Art. no. 2729.
- [24] G. Yang, J. Li, S. G. Zhou, and Y. Qi, "A wide-angle E-plane scanning linear array antenna with wide beam elements," *IEEE Antennas Wireless Propag. Lett.*, vol. 16, pp. 2923–2926, 2017.
- [25] G. Yang, J. Li, D. Wei, and R. Xu, "Study on wide-angle scanning linear phased array antenna," *IEEE Trans. Antennas Propag.*, vol. 66, no. 1, pp. 450–455, Jan. 2018.
- [26] H. Tian, L. J. Jiang, and T. Itoh, "A compact single-element pattern reconfigurable antenna with wide-angle scanning tuned by a single varactor," *Prog. Electromagn. Res. C*, vol. 92, pp. 137–150, 2019, doi: 10.2528/PIERC19021407.
- [27] Z. Jiang, S. Xiao, and Y. Li, "A wide-angle time-domain electronically scanned array based on energy-pattern-reconfigurable elements," *IEEE Antennas Wireless Propag. Lett.*, vol. 17, pp. 1598–1602, 2018.
- [28] K. Liu, S. Yang, S.-W. Qu, C. Chen, and Y. Chen, "Phased hemispherical lens antenna for 1-D wide-angle beam scanning," *IEEE Trans. Antennas Propag.*, vol. 67, no. 12, pp. 7617–7621, Dec. 2019.
- [29] G. Yang and S. Zhang, "Dual-polarized wide-angle scanning phased array antenna for 5G communication systems," *IEEE Trans. Antennas Propag.*, vol. 70, no. 9, pp. 7427–7438, Sep. 2022.
- [30] G. Yang, Y. Zhang, and S. Zhang, "Wide-band and wide-angle scanning phased array antenna for mobile communication system," *IEEE Open J. Antennas Propag.*, vol. 2, pp. 203–212, 2021.
- [31] A. Monti, S. Vellucci, M. Barbutto, D. Ramaccia, M. Longhi, C. Massagrande, A. Toscano, and F. Bilotti, "Quadratic-gradient metasurface-dome for wide-angle beam-steering phased array with reduced gain loss at broadside," *IEEE Trans. Antennas Propag.*, vol. 71, no. 2, pp. 2022–2027, Feb. 2023.
- [32] C.-Y.-D. Sim, H.-Y. Liu, and C.-J. Huang, "Wideband MIMO antenna array design for future mobile devices operating in the 5G NR frequency bands N77/N78/N79 and LTE band 46," *IEEE Antennas Wireless Propag. Lett.*, vol. 19, no. 1, pp. 74–78, Jan. 2020.
- [33] N. P. Kulkarni, N. Bhaskarrao Bahadure, P. D. Patil, and J. S. Kulkarni, "Flexible interconnected 4-port MIMO antenna for sub-6 GHz 5G and X band applications," *AEU-Int. J. Electron. Commun.*, vol. 152, Jul. 2022, Art. no. 154243.
- [34] S. K. Mahto, A. K. Singh, R. Sinha, M. Alibakhshienari, S. Khan, and G. Pau, "High isolated four element mimo antenna for ISM/LTE/5G (sub-6 GHz) applications," *IEEE Access*, vol. 11, pp. 82946–82959, 2023.
- [35] S. R. Thummaluru, M. Ameen, and R. K. Chaudhary, "Four-port MIMO cognitive radio system for midband 5G applications," *IEEE Trans. Antennas Propag.*, vol. 67, no. 8, pp. 5634–5645, Aug. 2019.
- [36] J. Sharad Kulkarni and C.-Y. Desmond Sim, "Low-profile, multiband & wideband 'C-shaped' monopole antenna for 5G and WLAN applications," in *Proc. Int. Conf. Radar, Antenna, Microw., Electron., Telecommun. (ICRAMET)*, Nov. 2020, pp. 366–371.
- [37] Y. Li, H. Zou, M. Wang, M. Peng, and G. Yang, "Eight-element MIMO antenna array for 5G/sub-6 GHz indoor micro wireless access points," in *Proc. Int. Workshop Antenna Technol. (iWAT)*, Mar. 2018, pp. 1–4.
- [38] S.-L. Chen, F. Wei, P.-Y. Qin, Y. J. Guo, and X. Chen, "A multi-linear polarization reconfigurable unidirectional patch antenna," *IEEE Trans. Antennas Propag.*, vol. 65, no. 8, pp. 4299–4304, Aug. 2017.

- [39] P.-Y. Qin, F. Wei, and Y. J. Guo, "A wideband-to-narrowband tunable antenna using a reconfigurable filter," *IEEE Trans. Antennas Propag.*, vol. 63, no. 5, pp. 2282–2285, May 2015.
- [40] J. Jiang, S. Yuan, and W. Zhang, "Design of ultrawideband planar monopole antenna of C shape," in *Proc. Int. Workshop Microw. Millim. Wave Circuits Syst. Technol.*, Oct. 2013, pp. 120–122.
- [41] Z. Ren, S. Wu, and A. Zhao, "Triple band MIMO antenna system for 5G mobile terminals," in *Proc. Int. Workshop Antenna Technol. (iWAT)*, Mar. 2019, pp. 163–165.
- [42] S. Dey, S. Dey, and S. K. Koul, "Isolation improvement of MIMO antenna using novel EBG and hair-pin shaped DGS at 5G millimeter wave band," *IEEE Access*, vol. 9, pp. 162820–162834, 2021.
- [43] U. N. Nissan and G. Singh, "Terahertz antenna for 5G cellular communication systems: A holistic review," in *Proc. IEEE Int. Conf. Microw., Antennas, Commun. Electron. Syst. (COMCAS)*, Nov. 2019, pp. 1–6.
- [44] M. Sung, J. Kim, E.-S. Kim, S.-H. Cho, Y.-J. Won, B.-C. Lim, S.-Y. Pyun, H. Lee, J. K. Lee, and J. H. Lee, "RoF-based radio access network for 5G mobile communication systems in 28 GHz millimeter-wave," *J. Lightw. Technol.*, vol. 38, no. 2, pp. 409–420, Jan. 15, 2020.
- [45] B. G. Kim, S. H. Bae, H. Kim, and Y. C. Chung, "RoF-based mobile fronthaul networks implemented by using DML and EML for 5G wireless communication systems," *J. Lightw. Technol.*, vol. 36, no. 14, pp. 2874–2881, Jul. 15, 2018.
- [46] N. O. Parchin, A. S. I. Amar, M. Darwish, K. H. Moussa, C. H. See, R. A. Abd-Alhameed, N. M. Alwadai, and H. G. Mohamed, "Four-element/eight-port MIMO antenna system with diversity and desirable radiation for sub 6 GHz modern 5G smartphones," *IEEE Access*, vol. 10, pp. 133037–133051, 2022.
- [47] G. P. Agrawal, *Fiber-Optic Communication Systems*. Hoboken, NJ, USA: Wiley, 2012.
- [48] A. J. Seeds and T. Ismail, "Broadband access using wireless over multi-mode fiber systems," *J. Lightw. Technol.*, vol. 28, no. 16, pp. 2430–2435, Aug. 15, 2010.
- [49] R. Azizpour, H. Zakeri, and G. Moradi, "Beam pattern control for graphene-based patch array antenna with radio-over-fiber systems by using modulation instability phenomenon," *Opt. Continuum*, vol. 2, no. 4, p. 865, Apr. 2023.
- [50] K. V. Babu, S. Das, G. N. J. Sree, S. K. Patel, M. P. Saradhi, and M. R. N. Tagore, "Design and development of miniaturized MIMO antenna using parasitic elements and machine learning (ML) technique for lower sub 6 GHz 5G applications," *AEU-Int. J. Electron. Commun.*, vol. 153, Aug. 2022, Art. no. 154281.
- [51] G.-H. Sun and H. Wong, "Circularly polarized elliptical cavity-backed patch antenna array for millimeter-wave applications," *IEEE Trans. Antennas Propag.*, vol. 70, no. 11, pp. 10512–10519, Nov. 2022.
- [52] H. Xue, R. Li, P. Xu, H. Liu, and L. Li, "Model construction, theoretical analysis, and miniaturized implementation of high-order deflected multivortex beams with uniform elliptical array," *IEEE Trans. Antennas Propag.*, vol. 70, no. 8, pp. 7234–7239, Aug. 2022.
- [53] N. C. Azenui and H. Y. D. Yang, "A printed crescent patch antenna for ultrawideband applications," *IEEE Antennas Wireless Propag. Lett.*, vol. 6, pp. 113–116, 2007.
- [54] H. Xue, H. Liu, Q. Shao, Q. Feng, and L. Li, "Double-deflection vortex beam generation using a single elliptical patch with the theory of characteristic modes," *Optics Exp.*, vol. 28, no. 8, pp. 12322–12330, 2020.
- [55] D. K. Raheja, S. Kumar, B. K. Kanaujia, S. K. Palaniswamy, R. R. Thipparaju, and M. Kanagasabai, "Truncated elliptical self-complementary antenna with quad-band notches for SWB MIMO systems," *AEU-Int. J. Electron. Commun.*, vol. 131, Mar. 2021, Art. no. 153608.
- [56] H. Zakeri, M. Parvaneh, and G. Moradi, "A compact RHCP and LHCP truncated corner patch series-fed array antenna," *Int. J. Electron. Lett.*, vol. 11, no. 1, pp. 125–133, Jan. 2023.
- [57] C. Li, X.-W. Zhu, P. Liu, C. Yu, and W. Hong, "A metasurface-based multilayer wideband circularly polarized patch antenna array with a parallel feeding network for Q-band," *IEEE Antennas Wireless Propag. Lett.*, vol. 18, no. 6, pp. 1208–1212, Jun. 2019.
- [58] B. Bismil and S. Azeem, "A survey on increasing the capacity of 5G fronthaul systems using RoF," *Opt. Fiber Technol.*, vol. 74, Dec. 2022, Art. no. 103078.
- [59] S. Shen, T. Zhang, S. Mao, and G.-K. Chang, "DRL-based channel and latency aware radio resource allocation for 5G service-oriented RoF-mmWave RAN," *J. Lightw. Technol.*, vol. 39, no. 18, pp. 5706–5714, Sep. 30, 2021.
- [60] A. J. Akbarfam and K. K. Motarjemi, "Proposing a new protocol for using device-to-device communications in narrowband IoT-based systems," in *Proc. 11th Smart Grid Conf. (SGC)*, Dec. 2021, pp. 1–5.
- [61] M. S. B. Cunha, E. S. Lima, N. Andriolli, D. H. Spadoti, G. Contestabile, and A. Cerqueira, "5G NR RoF system based on a monolithically integrated multi-wavelength transmitter," *IEEE J. Sel. Topics Quantum Electron.*, vol. 27, no. 2, pp. 1–8, Mar. 2021.
- [62] R. Hussain, M. U. Khan, and M. S. Sharawi, "An integrated dual MIMO antenna system with dual-function GND-plane frequency-agile antenna," *IEEE Antennas Wireless Propag. Lett.*, vol. 17, no. 1, pp. 142–145, Jan. 2018.
- [63] M. Ikram, N. Nguyen-Trong, and A. M. Abbosh, "Realization of a tapered slot array as both decoupling and radiating structure for 4G/5G wireless devices," *IEEE Access*, vol. 7, pp. 159112–159118, 2019.
- [64] Y. Liu, Y. Li, L. Ge, J. Wang, and B. Ai, "A compact hepta-band mode-composite antenna for sub (6, 28, and 38) GHz applications," *IEEE Trans. Antennas Propag.*, vol. 68, no. 4, pp. 2593–2602, Apr. 2020.
- [65] Y. Kumar, R. K. Gangwar, and B. K. Kanaujia, "Characterization of CP radiations in a planar monopole antenna using tuning fork fractal slot for LTE Band13/Wi-Max and Wi-Fi applications," *IEEE Access*, vol. 8, pp. 127123–127133, 2020.
- [66] N. A. Kudryashov, "Model of propagation pulses in an optical fiber with a new law of refractive indices," *Optik*, vol. 248, Dec. 2021, Art. no. 168160.
- [67] G. P. Agrawal, "Nonlinear fiber optics," in *Nonlinear Science at the Dawn of the 21st Century* (Lecture Notes in Physics), vol. 542, P. L. Christiansen, M. P. Sørensen, and A. C. Scott, Eds. Berlin, Germany: Springer, 2000, doi: 10.1007/3-540-46629-0_9.
- [68] E. Karooby, H. Sahbafar, M. H. Heris, A. Hadi, and V. Eskandari, "Identification of low concentrations of flucytosine drug using a surface-enhanced Raman scattering (SERS)-active filter paper substrate," *Plasmonics*, vol. 19, no. 2, pp. 855–863, Apr. 2024.
- [69] X. Xu, J. Wu, T. G. Nguyen, T. Moein, S. T. Chu, B. E. Little, R. Morandotti, A. Mitchell, and D. J. Moss, "Photonic microwave true time delays for phased array antennas using a 49 GHz FSR integrated optical micro-comb source [invited]," *Photon. Res.*, vol. 6, no. 5, p. B30, May 2018.



HASSAN ZAKERI was born in Rome, Italy, in 1996. He received the M.Sc. degree in electrical engineering from the Amirkabir University of Technology (Tehran Polytechnic), in 2021, where he is currently pursuing the Ph.D. degree with the Electromagnetic Research Laboratory, Electrical Engineering Department. His research interests include microwave photonic, antennas, optical fiber, 5G/6G and beyond wireless communications, and multiple input multiple output (MIMO) systems.



RASUL AZIZPOUR was born in Mazandaran, Iran, in 1995. He received the M.Sc. degree in electrical engineering from the Amirkabir University of Technology, in 2022. His research interests include microwave photonic, antennas, non-destructive evaluation, 5G/6G and beyond wireless communications, and multiple input multiple output (MIMO) systems.



PARSA KHODDAMI was born in Babol, Iran, in 1995. He received the M.S. degree in electrical engineering from the Amirkabir University of Technology (Tehran Polytechnic), in 2022. He was a Teaching Assistant and a Lecturer with the Electrical Engineering Department, Amirkabir University of Technology, in 2022 and 2023, respectively. His research interests include metasurface, deep learning, 5G, and antennas.



GHOLAMREZA MORADI (Senior Member, IEEE) received the B.Sc. degree from the University of Tehran, in 1989, and the Ph.D. degree in electrical engineering from the Amirkabir University of Technology (Tehran Polytechnic), Tehran, Iran, in 2002. From 1997 to 2005, he was a Faculty Member and the Head of research department with the Civil Aviation Technology College, Tehran, where he developed a standardized training package approved by CAO, as a two-year project. He was on a sabbatical leave from the University of Alberta, from June 2016 to February 2016. He has some research collaboration with the University of Dresden. He has taught and worked in various universities, including Iran University of Science and Technology, Air Science University, Islamic Azad University, and the University of Sistan and Baluchestan. He is currently a Professor with the Department of Electrical Engineering, Amirkabir University of Technology. He has conducted several research projects on active microwave circuits, planar antenna, 5G wave roagation modeling, bioimplants, and high frequency measurement techniques. During past two decades, he has supervised more than ten Ph.D. candidates, 60 M.Sc. students, and 90 B.Sc. students. Also, he has acted as a referee of over 250 graduate students. He has authored over ten books in his specialty, among them, *Active Transmission Lines* won the award of the national book of the year, in 2008. He has published and presented almost 200 papers in the refereed journals and international conferences. His main research interests include high frequency characterization of materials, numerical electromagnetics, microwave imaging, planar microwave/mmwave, and THz systems. He has served as a member of lecturers' promotion committee in various universities. He is the Vice-Chair of the Electromagnetics and Photonic Society of IEEE Iran Section. He acts as a reviewer in many IEEE journals, and other highly reputed periodicals and international conferences. He is one of the co-founders of MMWaTT conferences.



MOHAMMAD ALIBAKHSHIKENARI (Member, IEEE) was born in Mazandaran, Iran, in February 1988. He received the Ph.D. degree (with the European label) in electronics engineering from the University of Rome "Tor Vergata," Italy, in February 2020. From May 2018 to December 2018, he was a Ph.D. Visiting Researcher with the Chalmers University of Technology, Gothenburg, Sweden. His training during the Ph.D. research visit included a research stage with Swedish company "Gap Waves AB." From November 2016 to February 2020, during the Ph.D. program, he has attended in 13 European Doctoral Schools organized by various European universities and organizations, and he successfully achieved all the credits leading him to obtain the Ph.D. degree with the European label. From February 2020 to July 2021, he was a Postdoctoral Research Fellow with the University of Rome "Tor Vergata." Since July 2021, he has been with the Department of Signal Theory and Communications, Universidad Carlos III de Madrid (uc3m), Spain, as a Principal Investigator of the CONEX (CONnecting EXcellence)-Plus Talent Training Program and Marie Skłodowska-Curie Actions. From 2021 to 2022, he was a Lecturer of the electromagnetic fields and electromagnetic laboratory with uc3m. From December 2022 to May 2023, he has a six months industrial research visit with SARAS Technology Ltd., Leeds, U.K., aligned with his CONEX-Plus Talent Training Program and Marie Skłodowska-Curie Actions project. In addition, he has research visits each up to one-week in the following universities: (i) the University of Catania, Sicily, Italy, in May 2024, along with an invited lecturer entitled "Terahertz Antennas based on Metasurface and SIW" for master's and Ph.D. students, and postdoctoral researchers; (ii) the University of Messina, Sicily, Italy, in May 2024; (iii) the University of Bradford, West Yorkshire, U.K., in May 2023; (iv) and Edinburgh Napier University, Edinburgh, U.K., in April 2023. His research interests include electromagnetic systems, antennas and wave-propagations, metamaterials and

metasurfaces, sensors, synthetic aperture radars (SAR), 5G and beyond wireless communications, multiple input multiple output (MIMO) systems, RFID tag antennas, substrate integrated waveguides (SIWs), impedance matching circuits, microwave components, millimeter-waves and terahertz integrated circuits, gap waveguide technology, beamforming matrix, and reconfigurable intelligent surfaces (RIS), which led to publishing eight book chapters and more than 250 research papers in scientific journals and international conferences, including 42 in-person presentations (oral and poster) in 28 conferences and 26 on-line presentations in 12 conferences. These research activities helped him to achieve more than 6300 citations and H-index above 50 reported by Scopus, Google Scholar, and ResearchGate. He received the Teaching Excellent Acknowledgement Certificate for the course of electromagnetic fields from the Vice-Rector of studies. He was a recipient of the three years Principal Investigator Research Grant funded by the Universidad Carlos III de Madrid and the European Union's Horizon 2020 Research and Innovation Program under the Marie Skłodowska-Curie Grant, in July 2021; the two years postdoctoral research grant funded by the University of Rome "Tor Vergata," in November 2019; the three years Ph.D. Scholarship funded by the University of Rome "Tor Vergata," in November 2016; and the two Young Engineer Awards of the 47th and 48th European Microwave Conferences held in Nuremberg, Germany, in 2017, and in Madrid, Spain, in 2018, respectively. In April 2020, his research article titled "High-Gain Metasurface in Polyimide On-Chip Antenna Based on CRLH-TL for Sub Terahertz Integrated Circuits," [Scientific Reports, volume 10, Article number 4298 (2020)] was received the Best Month Paper at the University of Bradford, UK. He is an editor of the book project titled *Ultra-Wideband Technologies—Diverse Techniques and Applications* (IntechOpen, the world's leading publisher of Open Access books). He acts as a referee in several highly reputed journals and international conferences. In addition, he is a member of the reviewer panel of the Dutch Research Council (NWO) and U.K. Research and Innovation (UKRI) Funding Service, and also he was an external examiner of several Ph.D. dissertations from various universities. In addition, he serves as an Associate Editor for two scientific journals, such as *Radio Science* and *IET Journal of Engineering*.



CHAN HWANG SEE (Senior Member, IEEE) received the B.Eng. degree (Hons.) in electronic, telecommunication and computer engineering and the Ph.D. degree from the University of Bradford, U.K., in 2002 and 2007, respectively. He is a Professor of antennas and applied electromagnetics with the School of Computing, Engineering and the Built Environment, Edinburgh Napier University, U.K. From 2019 to 2022, he was the Head of electrical engineering and mathematics with Edinburgh Napier University. His research interests include wireless sensor network system design, computational bioelectromagnetics, antennas, microwave circuits, the Internet of Things (IoT), microwave sensors, wireless power transfer (WPT), and microwave energy harvesting. He has published over 250 peer-reviewed journal articles and conference papers in these research areas. He is the co-author of one book and three book chapters. He is a Chartered Engineer, a fellow of the Institution of Engineering and Technology and the Higher Education Academy, and a Full Member of the EPSRC Review College. He received the IEEE Malaysia AP/MTT/EMC Joint Chapter Best Paper Award, in 2020. He was a recipient of two Young Scientist Awards from the International Union of Radio Science (URSI) and Asia-Pacific Radio Science Conference (AP-RASC), in 2008 and 2010, respectively. He also received a certificate of excellence for his successful Knowledge Transfer Partnership (KTP) with Yorkshire Water on the design and implementation of a wireless sensor system for sewerage infrastructure monitoring, in 2009. Since 2023, he has been served as the U.K. Representative for Commission K: Electromagnetics in Biology and Medicine within International Union of Radio Science (URSI). He is an Associate Editor of IEEE Access; and an Editor of *Journal of Electronics and Electrical Engineering*, *Scientific Reports*, *PeerJ Computer Science*, *Frontiers in Antennas and Propagation—Metamaterial Antennas and Wireless Power Transfer*. According to Web of Science, he has completed over 500 verified reviews and over 250 verified editor records.



TAYEB A. DENIDNI (Fellow, IEEE) received the M.Sc. and Ph.D. degrees in electrical engineering from Laval University, Quebec City, QC, Canada, in 1990 and 1994, respectively. He was a Professor with the Department of Engineering, Université du Québec in Rimouski, Rimouski, QC, from 1994 to 2000, where he founded the Telecommunications Laboratory. Since 2000, he has been with the Institut National de la Recherche Scientifique (INRS), Université du Québec, Montreal, QC. He has founded the RF Laboratory with INRS-EM, Montreal. He has extensive experience in antenna design and is leading a large research group consisting of three research scientists, eight Ph.D. students, and two M.Sc. students. His current research interests include reconfigurable antennas using EBG and FSS structures, dielectric resonator antennas, metamaterial antennas, adaptive arrays, switched multibeam antenna arrays, ultra-wideband antennas, microwave, and development for wireless communications systems. He has served as an Associate Editor for IEEE ANTENNAS WIRELESS PROPAGATION LETTERS, from 2005 to 2007; and IEEE TRANSACTIONS ON ANTENNAS AND PROPAGATION, from 2008 to 2010. Since 2015, he has been serving as an Associate Editor for *IET Electronics Letters*.



FRANCISCO FALCONE (Senior Member, IEEE) received the degree in telecommunication engineering and the Ph.D. degree in communication engineering from the Universidad Pública de Navarra (UPNA), Spain, in 1999 and 2005, respectively. From February 1999 to April 2000, he was the Microwave Commissioning Engineer with Siemens-Italtel, deploying microwave access systems. From May 2000 to December 2008, he was a Radio Access Engineer with Telefónica Móviles, performing radio network planning and optimization tasks in mobile network deployment. In January 2009, as a Co-Founding Member, he has been the Director of Tafco Metawireless, a spin-off company from UPNA, until May 2009. In parallel, he was an Assistant Lecturer with the Electrical and Electronic Engineering Department, UPNA, from February 2003 to May 2009. In June 2009, he becomes an Associate Professor with the EE Department, being the Department Head, from January 2012 to July 2018. From January 2018 to May 2018, he was a Visiting Professor with Kuwait College of Science and Technology, Kuwait. He is also affiliated with the Institute for Smart Cities (ISC), UPNA, which hosts around 140 researchers. He is currently acting as the Head of the ICT Section. He has over 500 contributions in indexed international journals, book chapters, and conference contributions. His research interests include computational electromagnetics applied to the analysis of complex electromagnetic scenarios, with a focus on the analysis, design, and implementation of heterogeneous wireless networks to enable context-aware environments. He received the CST 2003 and CST 2005 Best Paper Award; the Ph.D. Award from the Colegio Oficial de Ingenieros de Telecomunicación (COIT), in 2006; the Doctoral Award UPNA, in 2010; the first Juan Gomez Peñalver Research Award from the Royal Academy of Engineering of Spain, in 2010; the XII Talgo Innovation Award, in 2012; the IEEE 2014 Best Paper Award, in 2014; the ECSA-3 Best Paper Award, in 2016; and the ECSA-4 Best Paper Award, in 2017.



SLAWOMIR KOZIEL (Fellow, IEEE) received the M.Sc. and Ph.D. degrees in electronic engineering from Gdańsk University of Technology, Poland, in 1995 and 2000, respectively, and the M.Sc. degree in theoretical physics and the M.Sc. and Ph.D. degrees in mathematics from the University of Gdańsk, Poland, in 2000, 2002, and 2003, respectively. He is currently a Professor with the Department of Technology, Reykjavik University, Iceland. His current research interests include the

CAD and modeling of microwave and antenna structures, simulation-driven design, surrogate-based optimization, space mapping, circuit theory, analog signal processing, evolutionary computation, and numerical analysis.



ERNESTO LIMITI (Senior Member, IEEE) has been a Full Professor of electronics with the Engineering Faculty, University of Roma “Tor Vergata,” since 2002. Since 1991, he has been a Research Assistant and a Teaching Assistant with the University of Roma “Tor Vergata,” where he has also been an Associate Professor, since 1998. He represents the University of Roma “Tor Vergata” in the governing body of the Microwave Engineering Center for Space Applications (MECSA), an inter-university center among several Italian universities. He has been elected to represent the Industrial Engineering Sector in the Academic Senate of the University, from 2007 to 2010 and from 2010 to 2013. He is the President of the Consortium “Advanced Research and Engineering for Space,” ARES, formed between the university and two companies. Further, he is the President of the Laurea and Laurea Magistrale degrees in electronic engineering with the University of Roma “Tor Vergata.” He is actively involved in research activities with many research groups, both European and Italian, and he is in tight collaborations with high-tech Italian (Selex-SI, Thales Alenia Space, Rheinmetall, Elettronica S.p.A., and Space Engineering) and foreign (OMMIC, Siemens, and UMS) companies. He has contributed, as a Researcher and/or unit responsible for several national (PRIN MIUR, Madess CNR, and Agenzia Spaziale Italiana) and international (ESPRIT COSMIC, Manpower, Edge, Special Action MEPI, ESA, EUROPA, Korrigan, RadioNet FP6, and FP7) projects. Regarding teaching activities, he teaches, over his institutional duties in the frame of the Corso di Laurea Magistrale in Ingegneria Elettronica, “Elettronica per lo Spazio” within the master’s course in Sistemi Avanzati di Comunicazione e Navigazione Satellitare. He is a member of the committee of the Ph.D. program in telecommunications and microelectronics with the University of Roma “Tor Vergata,” tutoring an average of four Ph.D. candidates per year. His research activity is focused on three main lines, all of them belonging to the microwave and millimetre-wave electronics research area. The first one is related to the characterization and modeling of active and passive microwave and millimetre-wave devices. Regarding active devices, the research line is oriented to the small-signal, noise, and large-signal modeling. Regarding passive devices, equivalent-circuit models have been developed for interacting discontinuities in microstrip, for typical MMIC passive components (MIM capacitors), and waveguide/coplanar waveguide transitions analysis and design. For active devices, new methodologies have been developed for the noise characterization and the subsequent modeling; and equivalent-circuit modeling strategies have been implemented both for small and large-signal operating regimes for GaAs, GaN, SiC, Si, InP MESFET/HEMT devices. The second line is related to design methodologies and characterization methods for low-noise circuits. The main focus is on cryogenic amplifiers and devices. Collaborations are currently ongoing with the major radioastronomy institutes all around Europe within the frame of FP6 and FP7 programs (RadioNet). Finally, the third line is in the analysis methods for nonlinear microwave circuits. In this line, novel analysis methods (spectral balance) are developed, together with the stability analysis of the solutions making use of traditional (harmonic balance) approaches. The above research lines have produced more than 250 publications in refereed international journals and presentations at international conferences. He acts as a referee of international journals of the microwave and millimetre wave electronics sector. He is on the steering committee of international conferences and workshops.

...

